J. Fluid Mech. (1985), *vol.* 160, *pp.* 297–315
Printed in Great Britain

Stability of finite-amplitude interfacial waves. Part 1. Modulational instability for small-amplitude waves

By R. H. J. GRIMSHAW
Department of Mathematics, University of Melbourne, Parkville, Vic 3052, Australia

AND D. I. PULLIN
Department of Mechanical Engineering, University of Queensland, St Lucia, Qld 4067, Australia

(Received 2 April 1984 and in revised form 7 November 1984)

In two previous papers (Pullin & Grimshaw 1983*a*, *b*) we studied the wave profile and other properties of finite-amplitude interfacial progressive waves in a two-layer fluid. In this and the following paper (Pullin & Grimshaw 1985) we discuss the stability of these waves to small perturbations. In this paper we obtain analytical results for the long-wavelength modulational instability of small-amplitude waves. Using a multiscale expansion, we obtain a nonlinear Schrödinger equation coupled to a wave-induced mean-flow equation to describe slowly modulated waves. From these coupled equations we determine the stability of a plane progressive wave. Our results are expressed by determining the instability bands in the (p, q)-plane, where (p, q) is the modulation wavenumber, and are obtained for a range of values of basic density ratio and undisturbed layer depths.

1. Introduction

It is well known that density-stratified fluids can support the propagation of waves. Large-amplitude internal waves are commonly observed on the oceanic pycnocline, or on atmospheric inversion layers. These waves have their largest amplitudes in the region where the basic density profile changes rapidly. Hence in two previous papers (Pullin & Grimshaw 1983*a*, *b*) we studied finite-amplitude interfacial progressive waves in a two-layer model in which the basic density is constant within each layer, but is discontinuous at the interface separating the layers, and in which there is a basic linear shear flow in the upper layer. The upper (lower) fluid has density ρ_1 (ρ_2) and is bounded above (below) by a rigid boundary at a distance d_1 (d_2) from the undisturbed interface; the basic flow in the upper layer is $\bar{u}_1 - \Omega_1 y$. Analytical results were obtained for small-amplitude waves from a third-order Stokes expansion. Numerical results were obtained for the special case when the lower layer is infinitely deep, using the Boussinesq approximation (i.e. the density difference across the interface is ignored except in the buoyancy term). It was shown that the wave profile is described by a nonlinear integral equation, which was solved numerically for a range of wave amplitudes up to the maximum amplitude.

In this and the following paper (Part 2 – Pullin & Grimshaw 1985) we shall discuss the stability of these waves to small perturbations for the case when there is no basic shear flow (i.e. $\bar{u}_1 = \Omega_1 = 0$). Yuen (1983) has studied the stability of interfacial waves when there is a basic current jump across the interface (i.e. $\bar{u}_1 \neq 0$, but $\Omega_1 = 0$), and

each layer is infinitely deep (i.e. $d_1, d_2 \to \infty$). The most noticeable difference between his results and ours is that, when $\bar{u}_1 \neq 0$, there is a short-wavelength Kelvin–Helmholtz instability for the undisturbed interface which persists for waves of small amplitude, although we note from Yuen's results that the low-order resonance instabilities of relatively long wavelength that we discuss below are also present when $\bar{u}_1 \neq 0$. In this paper we present analytical results for the long-wavelength modulational instability of small-amplitude waves, and in Part 2 we present numerical results for the instability of finite-amplitude waves for the special case when the lower layer is infinitely deep, using the Boussinesq approximation. These numerical results confirm that the long-wavelength modulational instability is part of a low-order resonance instability and persists for waves of moderate amplitude. In this respect our results are analogous to those obtained by McLean *et al.* (1981) and McLean (1982*a*, *b*) for surface gravity waves (i.e. $\rho_1 = 0$), and by Yuen (1983) for interfacial waves on infinitely deep layers (i.e. $d_1, d_2 \to \infty$).

Long-wavelength modulational instability of small-amplitude waves is best discussed within the context of the equations that govern slowly modulated small-amplitude waves. It has been shown by Grimshaw (1981) that, in general, for waves in stratified shear flows the modulation equation, for modulations in the same direction as the wave, is the nonlinear Schrödinger equation

$$\mathrm{i}\frac{\partial \eta_1}{\partial \tau} + \lambda_1 \frac{\partial^2 \eta_1}{\partial \xi^2} + \nu |\eta_1|^2 \eta_1 = 0, \tag{1.1a}$$

where

$$\tau = \epsilon^2 t, \quad \xi = \epsilon(x - Vt). \tag{1.1b}$$

Here $\epsilon\eta_1$ is the complex wave amplitude, and to leading order the wavetrain is described by $\epsilon\eta_1 \exp(\mathrm{i}kx - \mathrm{i}\omega t)$, where $\omega = \omega(k)$. The group velocity is $V = \partial\omega/\partial k$ and the coefficient $\lambda_1 = \frac{1}{2}\partial V/\partial k$. The coefficient ν of the nonlinear term is determined by the interactions of the second harmonic and the wave-induced mean flow with the primary wave. The derivation of (1.1*a*) requires that ϵ be a small parameter, and describes a balance between nonlinearity and wave dispersion about the dominant wavenumber k. It is well known that the nonlinear Schrödinger equation (1.1*a*) is a generic equation describing unidirectional wave modulation (see e.g. Benney & Newell 1967; Whitham 1974). In particular, it has been shown to describe the modulation of surface gravity waves (Zakharov 1968; Benney & Roskes 1969). Equation (1.1*a*) has the following plane-wave solution with amplitude A:

$$\eta_1 = A \exp(\mathrm{i}\nu |A|^2 \tau). \tag{1.2}$$

When this is subjected to modulational perturbations whose real and imaginary parts are proportional to

$$\mathrm{Re}\{\exp(s\tau + \mathrm{i}p\xi)\}, \tag{1.3}$$

then there is a modulational instability whenever $\lambda_1 \nu > 0$, and the growth rate s is given by

$$s^2 = \lambda_1 p^2 (2\nu |A|^2 - \lambda_1 p^2) \tag{1.4}$$

(see e.g. Davey & Stewartson 1974). There is instability for $0 < p^2 < 2\nu\lambda_1^{-1}|A|^2$, with a maximum growth rate of $\epsilon\nu|A|^2$ at $\lambda_1 p^2 = \nu|A|^2$.

When modulations transverse to the wave-propagation direction are also allowed, the general theory of Grimshaw (1981) shows that (1.1*a*) is replaced by

$$\mathrm{i}\frac{\partial \eta_1}{\partial \tau} + \lambda_1 \frac{\partial^2 \eta_1}{\partial \xi^2} + \lambda_2 \frac{\partial^2 \eta_1}{\partial Z^2} + \nu |\eta_1|^2 \eta_1 + Q\eta_1 = 0, \tag{1.5a}$$

where

$$Z = \epsilon z. \tag{1.5b}$$

Here $\lambda_2 = \frac{1}{2}V/k$, and Q is a variable representing that part of the wave-induced mean flow which responds to transverse modulations (i.e. to variations in Z). For the interfacial waves considered here we shall show that Q satisfies a linear fourth-order equation with a forcing term containing derivatives of $|\eta_1|^2$ (see (3.9a)). The resulting pair of equations is analogous to the pair of equations derived by Davey & Stewartson (1974) for transverse modulations of surface gravity waves. They reduce to the Davey–Stewartson equations when $\rho_1 = 0$. For modulations in a single direction defined by the modulation wavenumber (p, q) the coupled equations reduce to a single nonlinear Schrödinger equation of the same form as (1.1a) but with ξ replaced by $\xi_1 = p\xi + qZ$, λ_1 replaced by $\lambda = \lambda_1 p^2 + \lambda_2 q^2$ and ν replaced by $\nu + \hat{\nu}$, where $\hat{\nu}$ is a function of p and q. Instability criterion can now be derived in a manner similar to that described above. In particular, the growth rate s is given by an expression similar to (1.4) in which $\lambda_1 p^2$ is replaced by λ and ν is replaced by $(\nu + \hat{\nu})$. Instability now occurs for a band in the (p, q)-plane. The main purpose of this paper is to determine the configuration of these instability bands as a function of the density ratio ρ_1/ρ_2 and the non-dimensional depths kd_1 and kd_2.

The plan of this paper is as follows. In §2 we sketch the derivation of the modulation equation, and in §3 we derive the equations governing the wave-induced mean flow. Then in §4 we combine these two equations and determine the instability bands. Our results are presented, both analytically and graphically, for a range of values of ρ_1/ρ_2 and kd_1, kd_2. Finally, in §5 we present a brief discussion of the results. In particular, anticipating the numerical results of Part 2, we show the relationship between the modulational instability and an instability deriving from a low-order resonance.

2. Derivation of the modulation equation

We consider two incompressible and inviscid fluids separated by the interface $y = \eta(x, z, t)$. Gravity acts in the negative y-direction, and the fluid densities are ρ_1 and ρ_2, with $\rho_2 > \rho_1$, where subscripts 1 and 2 refer respectively to fluid properties above and below the interface. The fluid is bounded by horizontal planes at $y = d_1$ and $y = -d_2$. The basic unperturbed flow has a constant velocity $\bar{u}_1$ in the x-direction in the upper layer, $0 \leqslant y \leqslant d_1$, and a constant velocity $\bar{u}_2$ in the x-direction in the lower layer, $-d_2 \leqslant y \leqslant 0$. Although we shall put $\bar{u}_1 = \bar{u}_2 = 0$ in the subsequent application in §4, it is convenient to derive the modulation equations for the general case when $\bar{u}_1$, $\bar{u}_2$ are not zero. The perturbed flow is irrotational with a velocity potential $\phi_1(x, y, z, t)$ in the upper layer and $\phi_2(x, y, z, t)$ in the lower layer. The perturbed velocity field is then $\boldsymbol{u}_j = \nabla\phi_j$ $(j = 1, 2)$ with components (u_j, v_j, w_j), where $v_1 = 0$ at $y = d_1$ and $v_2 = 0$ at $y = -d_2$. It remains to specify the boundary conditions at the interface $y = \eta$. The two kinematic conditions are

$$\frac{\partial\eta}{\partial t} + \bar{u}_j \frac{\partial\eta}{\partial x} + u_j \frac{\partial\eta}{\partial x} + w_j \frac{\partial\eta}{\partial z} = v_j \quad (j = 1, 2) \quad \text{on } y = \eta. \tag{2.1}$$

Using the Bernoulli equation for each fluid, the dynamic boundary condition is

$$\rho_2\left(\frac{\partial\phi_2}{\partial t} + \bar{u}_2 \frac{\partial\phi_2}{\partial x} + \tfrac{1}{2}|\boldsymbol{u}_2|^2 + g\eta\right) - \rho_1\left(\frac{\partial\phi_1}{\partial t} + \bar{u}_1 \frac{\partial\phi_1}{\partial x} + \tfrac{1}{2}|\boldsymbol{u}_1|^2 + g\eta\right) = 0 \quad \text{on } y = \eta. \tag{2.2}$$

Plane-progressive periodic-wave solutions of (2.1) and (2.2) were discussed by Pullin & Grimshaw (1983a, b). Here we propose to discuss slowly modulated small-amplitude waves. A general theory for deriving modulation equations for stratified shear flows has been described by Grimshaw (1981). Indeed, the modulation

equation for the present case could be obtained from the general theory by making the appropriate substitutions. However, it is simpler to sketch how the general scheme works when applied to (2.1) and (2.2). First we introduce the small parameter ϵ, which describes both the slow modulations and the wave amplitude. Next we define the slow space and time variables by

$$X = \epsilon x, \quad Z = \epsilon z, \quad T = \epsilon t, \tag{2.3}$$

Modulated waves are then described by an expression of the form

$$\eta = \sum_{-\infty}^{\infty} \epsilon^{|n|} \eta_n(X, Z, T) \exp(in\theta), \quad \eta_{-n} = \eta_n^*, \tag{2.4a}$$

where

$$\theta = kx + lz - \omega t, \tag{2.4b}$$

and there are analogous expressions for ϕ_j. Here (k, l) is the wavenumber and ω is the frequency. Subsequently we assume that the wave is propagating in the x-direction and put $l = 0$, but it is convenient to retain l for the present development. After satisfying Laplace's equation in each fluid, the boundary conditions at $y = d_1$, $-d_2$ and the boundary conditions (2.1) and (2.2) at the interface, it may be shown that (see Grimshaw 1981)

$$\epsilon D(\hat{\omega}, \hat{k}, \hat{l})\, \eta_1 + N_1 = 0, \tag{2.5a}$$

where

$$D(\omega, k, l) = (\rho_2 - \rho_1) g - \rho_2 \frac{(\omega - k\bar{u}_2)^2}{\kappa} \coth \kappa d_2 - \rho_1 \frac{(\omega - k\bar{u}_1)^2}{\kappa} \coth \kappa d_1, \tag{2.5b}$$

$$\hat{\omega} = \omega + i\epsilon \frac{\partial}{\partial T}, \quad \hat{k} = k - i\epsilon \frac{\partial}{\partial X}, \quad \hat{l} = l - i\epsilon \frac{\partial}{\partial Z}. \tag{2.5c}$$

Here N_1 represents nonlinear terms. When these have been specified, (2.5a) is the required modulation equation.

It can be shown that the nonlinear term N_1 is $O(\epsilon^3)$. Hence, to leading order in ϵ, (2.5a) reduces to $D(\omega, k, l) = 0$, which is just the dispersion relation for a linear plane progressive wave. Expanding the operator $D(\hat{\omega}, \hat{k}, \hat{l})$ in powers of ϵ, it is readily shown that, to leading order, modulations propagate with the group velocity (V, W), where

$$V = \frac{\partial \omega}{\partial k}, \quad W = \frac{\partial w}{\partial l}. \tag{2.6}$$

In order to continue the expansion to $O(\epsilon^3)$ we introduce the long-time variable

$$\tau = \epsilon T = \epsilon^2 t. \tag{2.7}$$

We shall also now suppose that $l = 0$ and the wave is propagating in the x-direction; it follows that $W = 0$. It is convenient to choose a frame of reference moving with the group velocity, and hence we put

$$\xi = X - VT, \tag{2.8}$$

and seek solutions of (2.5a) for which $\eta_1 = \eta_1(\xi, Z, \tau)$. It can be shown that (2.5a) becomes, to $O(\epsilon^3)$,

$$i\epsilon^3 D_\omega \frac{\partial \eta_1}{\partial \tau} + \tfrac{1}{2}\epsilon^3 D_\omega \left(\frac{\partial V}{\partial k} \frac{\partial^2 \eta_1}{\partial \xi^2} + \frac{\partial W}{\partial l} \frac{\partial^2 \eta_1}{\partial Z^2} \right) + N_1 = 0. \tag{2.9}$$

Here we recall that the coefficients D etc. are evaluated at $l = 0$. For future use we note that, at $l = 0$,

$$\frac{\partial W}{\partial l} = \frac{V}{k} + \frac{1}{k^2 D_\omega}\left(\bar{u}_1 \frac{\partial D}{\partial \bar{u}_1} + \bar{u}_2 \frac{\partial D}{\partial \bar{u}_2}\right). \tag{2.10}$$

Here the partial derivates of D with respect to $\bar{u}_j$ are obtained from (2.5*b*), keeping ω, k and l and all other parameters fixed.

From the general theory of Grimshaw (1981) the nonlinear term N_1 is made up of two parts. One part contains the interaction of the second harmonic (i.e. terms such as η_2) with the primary harmonic η_1, together with the cubic interactions of η_1; it is identical with the same term that arises in the Stokes expansion for a plane progressive wave and will be denoted by $N_1^{(2)}$. The other part contains the interactions of the wave-induced mean flow (i.e. terms such as η_0) with the primary harmonic η_1, and will be denoted by $N_1^{(0)}$. We find that, to $O(\epsilon^3)$,

$$N_1 = \epsilon^3 (N_1^{(2)} + N_1^{(0)}), \tag{2.11a}$$

where

$$N_1^{(2)} = \nu_2 |\eta_1|^2 \eta_1, \tag{2.11b}$$

$$N_1^{(0)} = \left(\frac{\partial D}{\partial d_2} - \frac{\partial D}{\partial d_1}\right)\eta_0 \eta_1 + \frac{\partial D}{\partial \bar{u}_1} u_0^{(1)} \eta_1 + \frac{\partial D}{\partial \bar{u}_2} u_0^{(2)} \eta_1. \tag{2.11c}$$

Here $u_0^{(j)}$ ($j = 1, 2$) are the $O(\epsilon^2)$ wave-induced mean velocities in the x-direction, and we have replaced η_0 by $\epsilon^2 \eta_0$. The coefficient ν_2 in (2.11*b*), being identical with that in the Stokes expansion, was obtained by Pullin & Grimshaw (1983*a*). For convenience we quote the result here:

$$\nu_2 = k^3 \left\{ \frac{[\rho_2 (c-\bar{u}_2)^2 (3S_2^2 - 1) - \rho_1 (c-\bar{u}_1)^2 (3S_1^2 - 1)]^2}{2[\rho_2 (c-\bar{u}_2)^2 / S_2 + \rho_1 (c-\bar{u}_1)^2 / S_1]} \right.$$
$$\left. - 2\rho_2 (c-\bar{u}_2)^2 S_2 (S_2^2 - 2) - 2\rho_1 (c-\bar{u}_1)^2 S_1 (S_1^2 - 2) \right\}, \tag{2.12a}$$

where

$$S_j = \coth k d_j \quad (j = 1, 2), \quad \omega = kc. \tag{2.12b}$$

The modulation equation is obtained by substituting (2.11*a–c*) into (2.9). To complete it, we must obtain the equations determining the wave-induced mean flow η_0, $u_0^{(1)}$ and $u_0^{(2)}$. This aspect is discussed in §3.

3. Wave-induced mean flow

The mean-flow equations are those for the $n = 0$ components in the expansions (2.4*a*, *b*). They are most readily obtained by averaging (2.1) and (2.2) over the phase θ. First, however, we note that, since $\phi_0^{(j)}(X, Z, T; y)$ satisfies Laplace's equation,

$$\phi_0^{(j)} = \epsilon \Phi_0^{(j)}(X, Z, T) + O(\epsilon^3), \tag{3.1a}$$

$$u_0^{(j)} = \frac{\partial \Phi_0^{(j)}}{\partial X}, \quad w_0^{(j)} = \frac{\partial \Phi_0^{(j)}}{\partial Z}. \tag{3.1b}$$

Here, in (3.1*b*), $O(\epsilon^2)$ error terms have been omitted; note that the wave-induced velocities $u_0^{(j)}$ and $w_0^{(j)}$ are independent of y to leading order. Averaging the kinematic

boundary conditions yields the equations

$$\frac{\partial \eta_0}{\partial T}+\bar{u}_j\frac{\partial \eta_0}{\partial X}\mp d_j\frac{\partial u_0^{(j)}}{\partial X}\mp d_j\frac{\partial w_0^{(j)}}{\partial Z}\mp\frac{\partial F_0^{(j)}}{\partial X}\mp\frac{\partial G_0^{(j)}}{\partial Z}=0, \tag{3.2a}$$

where

$$\rho_j F_0^{(j)}=\frac{\partial D}{\partial \bar{u}_j}|\eta_1|^2, \tag{3.2b}$$

$$\rho_j G_0^{(j)}=\frac{l}{k}\frac{\partial D}{\partial \bar{u}_j}|\eta_1|^2. \tag{3.2c}$$

Here we have omitted error terms $O(\epsilon^2)$, and the alternate signs refer to $j=1, 2$. Averaging the dynamic boundary condition gives the equation, correct to $O(\epsilon^2)$,

$$\rho_2\left(\frac{\partial \Phi_0^{(2)}}{\partial T}+\bar{u}_2\frac{\partial \Phi_0^{(2)}}{\partial X}+g\eta_0\right)-\rho_1\left(\frac{\partial \Phi_0^{(1)}}{\partial T}+\bar{u}_1\frac{\partial \Phi_0^{(1)}}{\partial X}+g\eta_0\right)+H_0=0, \tag{3.3a}$$

where

$$H_0=\left(\frac{\partial D}{\partial d_2}-\frac{\partial D}{\partial d_1}\right)|\eta_1|^2. \tag{3.3b}$$

The mean-flow equations are thus (3.2a) and (3.3a) for the mean-flow variables η_0 and $\Phi_0^{(j)}$.

To make further progress we now put $l=0$ and note that then $G_0^{(j)}$ (3.2c) vanishes. To leading order in ϵ the forcing terms in (3.2a) and (3.3a) are functions of $\xi=X-VT$ alone (see (2.8)), and hence we may find the forced solution by putting $\partial/\partial T=-V\partial/\partial X$ in (3.2a) and (3.3a). The free solutions of (3.2a) and (3.3a) are linear long waves which propagate at the linear long-wave phase speed c_0, which satisfies (2.11) in the limit $k\to 0$ (i.e. $D(kc_0, k, 0)\to 0$ as $k\to 0$). Since we shall assume that there is no long-wave resonance (i.e. $c_0\neq V$), which is the case for all k when $\bar{u}_1=\bar{u}_2=0$, these free long waves will separate from the wave modulations, which propagate at speed V, and will be ignored henceforth. Next we put

$$u_0^{(j)}=-\frac{1}{d_j}F_0^{(j)}\pm\frac{(\bar{u}_j-V)\eta_0}{d_j}+\hat{u}_0^{(j)}. \tag{3.4}$$

Recalling that $\partial/\partial T=-V\partial/\partial X$, we find that (3.2$a$) then becomes

$$\frac{\partial \hat{u}_0^{(j)}}{\partial X}+\frac{\partial w_0^{(j)}}{\partial Z}=0. \tag{3.5}$$

Further, on substituting (3.4) into (3.3a), we find that

$$D_0(V)\hat{\eta}_0+\rho_2(\bar{u}_2-V)\hat{u}_0^{(2)}-\rho_1(\bar{u}_1-V)\hat{u}_0^{(1)}=0, \tag{3.6a}$$

where

$$\eta_0=\frac{I_0}{D_0(V)}|\eta_1|^2+\hat{\eta}_0, \tag{3.6b}$$

$$I_0=-\left(\frac{\partial D}{\partial d_2}-\frac{\partial D}{\partial d_1}\right)+\frac{\bar{u}_2-V}{d_2}\frac{\partial D}{\partial \bar{u}_2}-\frac{\bar{u}_1-V}{d_1}\frac{\partial D}{\partial \bar{u}_1}, \tag{3.6c}$$

$$D_0(V)=(\rho_2-\rho_1)g-\frac{\rho_2}{d_2}(\bar{u}_2-V)^2-\frac{\rho_1}{d_1}(\bar{u}_1-V)^2. \tag{3.6d}$$

Note that $D_0(V)$ is the limit as $k\to 0$ of $D(kV, k, 0)$ and does not vanish, since $c_0\neq V$. Eliminating $w_0^{(j)}$ from (3.5), we find that

$$\frac{\partial^2 \hat{u}_0^{(j)}}{\partial X^2}+\frac{\partial^2 \hat{u}_0^{(j)}}{\partial Z^2}\pm\frac{\bar{u}_j-V}{d_j}\frac{\partial^2 \hat{\eta}_0}{\partial Z^2}=\left\{\frac{1}{\rho_j d_j}\frac{\partial D}{\partial \bar{u}_j}\mp\frac{\bar{u}_j-V}{d_j}\frac{I_0}{D_0}\right\}\frac{\partial^2|\eta_1|^2}{\partial Z^2}. \tag{3.7}$$

Finally, substituting (3.4) and (3.6*b*) into (2.11*c*), we find that

$$N_1^{(0)} = \nu_0 |\eta_1|^2 \eta_1 + \hat{N}_1^{(0)}, \tag{3.8a}$$

where

$$\nu_0 = -\frac{I_0^2}{D_0} - \frac{1}{\rho_1 d_1}\left(\frac{\partial D}{\partial \bar{u}_1}\right)^2 - \frac{1}{\rho_2 d_2}\left(\frac{\partial D}{\partial \bar{u}_2}\right)^2, \tag{3.8b}$$

$$\hat{N}_1^{(0)} = D_\omega Q \eta_1, \tag{3.8c}$$

$$D_\omega Q = -I_0 \hat{\eta}_0 + \frac{\partial D}{\partial \bar{u}_1}\hat{u}_0^{(1)} + \frac{\partial D}{\partial \bar{u}_2}\hat{u}_0^{(2)}. \tag{3.8d}$$

Thus the nonlinear term N_1 (2.11*a*) in the modulation equation has been reduced to cubic terms in η_1 alone, and $\hat{N}_1^{(0)}$, which is related to η_1 by (3.8*c*, *d*) and the long-wave equations (3.6*a*) and (3.7). In these latter equations the only forcing term is the transverse derivative (i.e. the Z-derivative) of $|\eta_1|^2$. The manipulations described above have removed the forcing terms due to modulations in the X-direction; their effect now appears in the coefficient ν_0 (3.8*b*) which is always negative. By cross-differentiation between (3.6*a*) and (3.7), we can obtain the following equation for Q alone:

$$D_\omega\left\{D_0\frac{\partial^2}{\partial X^2} + g(\rho_2 - \rho_1)\frac{\partial^2}{\partial Z^2}\right\}\left\{\frac{\partial^2 Q}{\partial X^2} + \frac{\partial^2 Q}{\partial Z^2}\right\} = \left[D_0\mu_1\frac{\partial^2}{\partial Z^2}\left\{\frac{\partial^2}{\partial X^2} + \frac{\partial^2}{\partial Z^2}\right\} + \mu_2\frac{\partial^4}{\partial Z^4}\right]|\eta_1|^2, \tag{3.9a}$$

where

$$\mu_1 = \frac{1}{\rho_1 d_1}\left\{\frac{\partial D}{\partial \bar{u}_1} - \frac{\rho_1 I_0(\bar{u}_1 - V)}{D_0}\right\}^2 + \frac{1}{\rho_2 d_2}\left\{\frac{\partial D}{\partial \bar{u}_2} + \frac{\rho_2 I_0(\bar{u}_2 - V)}{D_0}\right\}^2, \tag{3.9b}$$

$$\mu_2 = \frac{1}{\rho_1\rho_2 d_1 d_2}\left\{\rho_1(\bar{u}_1 - V)\frac{\partial D}{\partial \bar{u}_2} + \rho_2(\bar{u}_2 - V)\frac{\partial D}{\partial \bar{u}_1}\right\}^2. \tag{3.9c}$$

Note that both μ_1 and μ_2 are positive and satisfy the following relation, which is useful for subsequent computations:

$$\mu_1\{g(\rho_2 - \rho_1) - D_0\} = \mu_2 + \left\{\frac{I_0 g(\rho_2 - \rho_1)}{D_0} + \frac{\partial D}{\partial d_2} - \frac{\partial D}{\partial d_1}\right\}^2. \tag{3.10}$$

4. Modulational instability

The modulation equation is thus (2.9), where the nonlinear term N_1 is given by (2.11*a*, *b*) and (3.8*a*, *c*). It is coupled to the mean-flow equation for Q, (3.9*a*). Henceforth we shall put $\bar{u}_1 = \bar{u}_2 = 0$ and assume that the wave is propagating to the right, so that c, $V > 0$. The modulation equation then becomes (1.5*a*). For the convenience of the reader we reproduce that equation here, and note that the coefficients λ_1, λ_2 can be identified from (2.9) and (2.10):

$$\mathrm{i}\frac{\partial \eta_1}{\partial \tau} + \lambda_1\frac{\partial^2 \eta_1}{\partial \xi^2} + \lambda_2\frac{\partial^2 \eta_1}{\partial Z^2} + \nu|\eta_1|^2\eta_1 + Q\eta_1 = 0, \tag{4.1a}$$

where

$$D_\omega \nu = \nu_2 + \nu_0, \tag{4.1b}$$

$$\lambda_1 = \frac{1}{2}\frac{\partial V}{\partial k}, \quad \lambda_2 = \frac{V}{2k}. \tag{4.1c}$$

Here we recall that ν_2 is defined by (2.12*a*) and ν_0 by (3.8*b*). If we put $\rho_1 = 0$, then

(4.1a) and (3.9a) reduce to the Davey–Stewartson equations for the modulation of a surface gravity wave (Davey & Stewartson 1974). In order to use (4.1a) and (3.9a) to describe modulational instability, we first seek solutions corresponding to modulations in a single direction specified by the modulation wavenumber (p, q). Thus we put

$$\xi_1 = p\xi + qZ \tag{4.2}$$

and seek solutions for which η_1 and Q are functions of τ and ξ_1 only. We find from (3.9a) that

$$Q = \hat{\nu}\,|\eta_1|^2, \tag{4.3a}$$

where

$$D_\omega(p^2+q^2)\,(D_0 p^2 + g(\rho_2-\rho_1)\,q^2)\,\hat{\nu} = q^2(D_0\mu_1(p^2+q^2)+\mu_2 q^2). \tag{4.3b}$$

Substituting (4.2a) and (4.3a) into (4.1a), we obtain the nonlinear Schrödinger equation

$$\mathrm{i}\frac{\partial\eta_1}{\partial\tau} + \lambda\frac{\partial^2\eta_1}{\partial\xi_1^2} + (\nu+\hat{\nu})\,|\eta_1|^2\eta_1 = 0, \tag{4.4a}$$

where

$$\lambda = \lambda_1 p^2 + \lambda_2 q^2. \tag{4.4b}$$

The modulational instability is now found by perturbing the plane-wave solution of (4.4a). For modulations in the wave direction the results are described by (1.2), (1.3) and (1.4). When the modulation is transverse ($q \neq 0$) the necessary modifications have been described in §1, and for the convenience of the reader are described below. The plane-wave solution of (4.4a) is

$$\eta_1 = A\exp(\mathrm{i}(\nu+\hat{\nu})\,|A|^2\tau). \tag{4.5}$$

When $q = 0$, so that $\hat{\nu} = 0$, this is just the plane progressive wave. When this is subjected to modulational perturbations whose real and imaginary parts are proportional to

$$\mathrm{Re}\{\exp(s\tau + \mathrm{i}\xi_1)\}, \tag{4.6}$$

then there is modulational instability whenever $\lambda(\nu+\hat{\nu}) > 0$, and the growth rate s is given by

$$s^2 = \lambda(2(\nu+\hat{\nu})\,|A|^2 - \lambda). \tag{4.7}$$

The stability boundaries in the (p,q)-plane are given by $\lambda = 0$ and $\lambda = 2(\nu+\hat{\nu})\,|A|^2$, while the maximum growth rate is $(\nu+\hat{\nu})\,|A|^2$ and occurs at $\lambda = (\nu+\hat{\nu})\,|A|^2$. Since s (4.7) is symmetric in p and q, it is sufficient to consider the quadrant $p \geqslant 0$, $q \geqslant 0$. We note here that $\lambda_1 < 0$ and $\lambda_2 > 0$, so that the boundary $\lambda = 0$ is a straight line through the origin in the (p,q)-plane. Also $D_\omega < 0$ and $\nu_0 < 0$ (3.8b); however, ν_2 (2.12a) can take either sign. Thus, although ν is independent of p and q, it can take either sign. On the other hand, although $\hat{\nu}$ (4.3b) depends on p and q, $\hat{\nu} < 0$, since $D_\omega < 0$, $D_0 > 0$ (3.6d), and μ_1 (3.9b) and μ_2 (3.9c) are both positive. The various combinations of signs lead to four possible configurations for the instability bands in the (p,q)-plane. These are shown in figure 1. If $\nu < 0$ then the configuration is similar to that for deep-water surface gravity waves and is shown in figure 1 (a). If $\nu > 0$ but $(\nu+\hat{\nu}) < 0$ when $p = 0$ then the configuration is either that of figure 1 (b) or (c); figure 1 (b) occurs when the zero of $\nu+\hat{\nu}$ as a function of the slope q/p leads to a slope less than that defined by $\lambda = 0$, while figure 1 (c) occurs in the contrary case. If $\nu = 0$ and $\nu+\hat{\nu} > 0$ when $p = 0$ then the configuration is that of figure 1 (d), since it can be shown that now $\nu+\hat{\nu}$, considered as a function of the slope q/p has no zeros. Hereinafter we shall refer to these diagrams as case A, B, C or D respectively. Cases A, B and C all occur for surface gravity waves (i.e. $\rho_1 = 0$, see Benney & Roskes 1969).

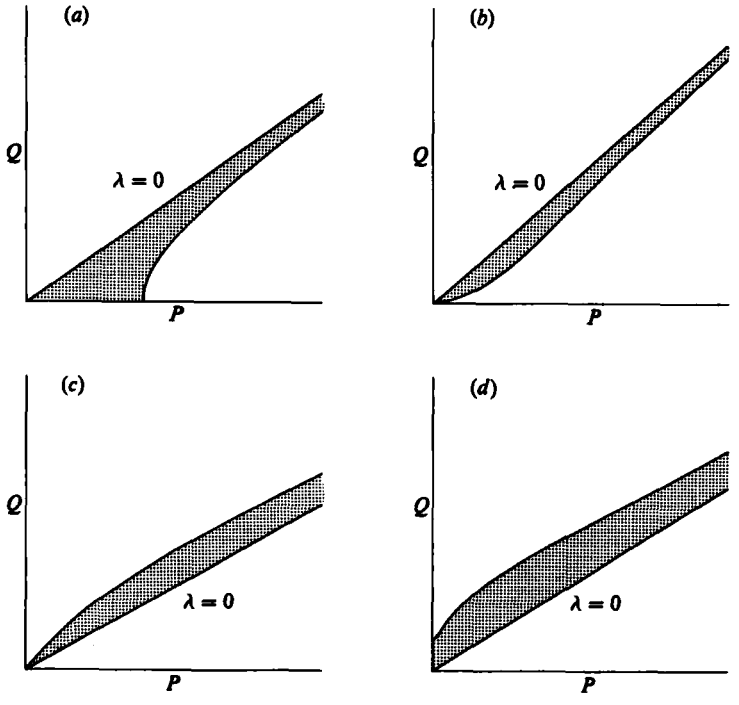

FIGURE 1. Configuration of instability bands in (P,Q)-plane for modulational instability of interfacial waves. Shaded regions are unstable bands; the $\lambda = 0$ boundary is as indicated. (*a*) Case A; (*b*) B; (*c*) C; (*d*) D.

Of the various possibilities shown in figure 1, the instability configuration that actually occurs depends on the dimensionless parameters kd_1, kd_2 and ρ_1/ρ_2. Consider first the case when kd_1, $kd_2 \to \infty$, which is analogous to deep-water surface gravity waves. We find that

$$c^2 = \frac{g}{k}\frac{\rho_2-\rho_1}{\rho_2+\rho_1}, \quad V = \tfrac{1}{2}c, \tag{4.8a}$$

$$\lambda_1 = -\frac{c}{8k}, \quad \lambda_2 = \frac{c}{4k}. \tag{4.8b}$$

Hence the instability boundary $\lambda = 0$ is just $p = 2\frac{1}{2}q$. Further, η_0 and $u_0^{(2)} \to 0$ as kd_1, $kd_2 \to \infty$, so that $\nu_0 = 0$ and $\hat{\nu} = 0$, while ν is given by

$$\nu = -\frac{2ck^3(\rho_1^2+\rho_2^2)}{(\rho_1+\rho_2)^2}. \tag{4.9}$$

The other instability boundary is thus $\lambda = 2\nu|A|^2$ and is a hyperbola in the (p,q)-plane. The instability configuration is case A, which is shown in figure 1 (*a*).

Next, consider the opposite limit of shallow-water interfacial waves when kd_1, $kd_2 \to 0$. (Strictly speaking, the modulation equations are only valid in this limit when $\epsilon \ll (kd_1)^2, (kd_2)^2$, and hence restricted to very small amplitudes.) In this limit c, $V \to c_0$, where the long-wave phase speed is given by

$$c_0^2 = \frac{g(\rho_2-\rho_1)}{\rho_1/d_1+\rho_2/d_2}. \tag{4.10}$$

Also, we find that

$$\lambda_1 = -\tfrac{1}{2}kc_0\frac{\rho_2 d_1+\rho_2 d_2}{\rho_1/d_1+\rho_2/d_2}, \quad \lambda_2 = \frac{c_0}{2k} \tag{4.11}$$

In the shallow-water limit it is generally true that $\nu_2 = -\frac{1}{2}\nu_0$ (Grimshaw 1981, 1982), and hence there is stability to modulations in the wave direction ($q = 0$). We find that

$$\nu = \frac{9c_0}{4k}\frac{(\rho_2/d_2^2-\rho_1/d_1^2)^2}{(\rho_1 d_1+\rho_2 d_2)(\rho_1/d_1+\rho_2/d_2)}. \tag{4.12}$$

Further, we find that in this limit

$$D_0(V) = k^2c_0^2(\rho_1 d_1+\rho_2 d_2), \tag{4.13}$$

while $D_0\mu_1 \gg \mu_2$. Evaluating μ_1 from (3.9b) and substituting into (4.3b), we find that

$$\hat{\nu} = -2\nu\frac{q^2}{q^2+k^2p^2(\rho_1 d_1+\rho_2 d_2)(\rho_1/d_1+\rho_2/d_2)^{-1}}. \tag{4.14}$$

Thus the instability boundaries $\lambda = 0$ and $\lambda = 2(\nu+\hat{\nu})|A|^2$ collapse into the same straight line, which lies very close to the p-axis. However, the growth rate s tends to zero in this limit. The instability configuration is either case B or case C, where in the limit the two boundaries have coalesced. We conclude that shallow-water interfacial waves are modulationally stable, except possibly for wavenumbers (p, q) that lie close to the line $\lambda = 0$. This case is analogous to shallow-water surface gravity waves. Note that when $\rho_2 d_1^2 = \rho_2 d_2^2$, ν and $\hat{\nu}$ vanish in this approximation; to obtain the instability configuration higher-order terms must be calculated. Our numerical results, which are described below, indicate that the instability configuration is case D when $\rho_2 d_1^2 = \rho_1 d_2^2$.

Next we consider the case when the upper layer is deep and the lower layer is shallow, corresponding to the limits $kd_2 \to \infty$, followed by $kd_1 \to 0$. (Strictly speaking, the modulation equations are only valid in this limit when $\epsilon \ll (kd_1)$, and hence restricted to very small amplitudes.) In this limit the phase speed and group velocity are given by

$$c \approx c_0\left\{1-\frac{1}{2}\frac{\rho_2}{\rho_1}kd_1+k^2d_1^2\left(-\frac{1}{6}+\frac{3}{8}\frac{\rho_2^2}{\rho_1^2}\right)+O(k^3d_1^3)\right\}, \tag{4.15a}$$

$$V \approx c_0\left\{1-\frac{\rho_2}{\rho_1}kd_1+k^2d_1^2\left(-\frac{1}{2}+\frac{9}{8}\frac{\rho_2^2}{\rho_1^2}\right)+O(k^3d_1^3)\right\}, \tag{4.15b}$$

$$c_0^2 = \frac{gd_1(\rho_2-\rho_1)}{\rho_1}. \tag{4.15c}$$

Further, we find that

$$\lambda_1 \approx -\tfrac{1}{2}c_0\frac{\rho_2}{\rho_1}d_1, \quad \lambda_2 \approx \frac{c_0}{2k}, \tag{4.16a}$$

while

$$D_0(V) \approx g(\rho_2-\rho_1)\left\{2\frac{\rho_2}{\rho_1}kd_1+k^2d_1^2\left(1-\frac{13}{4}\frac{\rho_2^2}{\rho_1^2}\right)\right\}. \tag{4.16b}$$

Evaluating ν_2 from (2.12a) and ν_0 from (3.8b), we find that

$$\nu_2 \approx \frac{9}{2}\frac{\rho_1^2}{\rho_2}\frac{k^3c^2}{(kd_1)^4}\left\{1-kd_1\left(\frac{\rho_1}{\rho_2}+\frac{4}{9}\frac{\rho_2}{\rho_1}\right)\right\}, \tag{4.17a}$$

$$\nu_0 \approx -\frac{9}{2}\frac{\rho_1^2}{\rho_2}\frac{k^3c^2}{(kd_1)^4}\left\{1-kd_1\left(\frac{1}{2}\frac{\rho_1}{\rho_2}-\frac{61}{72}\frac{\rho_2}{\rho_1}\right)\right\}. \tag{4.17b}$$

Note that to leading order $\nu_2 = -\nu_0$, a result that is generally true in this limit (Grimshaw 1982). Thus stability to modulations in the wave direction ($q = 0$) is not determined by the leading-order terms in ν_2 and ν_0, and hence we have included the $O(kd_1)$ correction terms in (4.17*a*, *b*). From (4.1*b*) we find that

$$\nu \approx \frac{9}{8}\frac{kc_0}{d_1^2}\frac{\rho_1}{\rho_2}\left(\frac{\rho_1}{\rho_2}+\frac{31}{12}\frac{\rho_2}{\rho_1}\right). \tag{4.18}$$

Here, $\nu > 0$ and there is modulational stability in the wave direction ($q = 0$). Evaluating μ_1 and μ_2 from (3.9*b*, *c*), we find that $\mu_2 \to 0$ and $\hat{\nu}$ (4.3*b*) is given by

$$\hat{\nu} \approx -\frac{9}{4}\frac{c_0}{d_1^3}\frac{\rho_1}{\rho_2}\left\{\frac{q^2}{q^2+2kd_1(\rho_2/\rho_1)p^2}\right\}. \tag{4.19}$$

Thus the instability configuration is case B, where the instability boundaries $\lambda = 0$ and $\lambda = 2(\nu+\hat{\nu})|A|^2$ both lie very close to the p-axis. Unlike the shallow-water limit, the instability boundaries remain distinct and the growth rate s is not zero.

Another case that lends itself to some analytical simplification is $d_1 = d_2$ in the Boussinesq approximation, when $\rho_1 = \rho_2$ except in the combination $g(\rho_2-\rho_1)$. In this case we find that

$$c^2 = \frac{g(\rho_2-\rho_1)}{2\rho_1 kS_1}, \tag{4.20a}$$

$$V = \tfrac{1}{2}c\left\{1+\frac{kd_1(S_1^2-1)}{S_1}\right\}. \tag{4.20b}$$

Evaluating ν from (4.1*b*) using (2.12*a*) and (3.8*b*), we find that

$$\nu = ck^3\left\{(S_1^2-2)+\frac{2S_1}{kd_1}\right\}. \tag{4.21}$$

In this special case $I_0 = 0$, and hence it follows from (3.9*b*, *c*) that $\mu_2 = 2\rho_1 V^2\mu_1 d_1^{-1}$, with the consequence that $\hat{\nu}$ (4.3*b*) is given by

$$\hat{\nu} = -\frac{2ck^3S_1}{kd_1}\frac{q^2}{p^2+q^2}. \tag{4.22}$$

From these expressions for ν and $\hat{\nu}$ it is readily shown that as kd_1 is decreased there is a transition from case A to case B when $kd_1 = 2.17$ (i.e. when ν vanishes), to case C when $kd_1 = 1.51$, and finally to case D when $kd_1 = 0.88$ (i.e. when $\nu+\hat{\nu}$ vanishes for $p = 0$, or when $S_1^2 = 2$). The instability configuration remains in case D as $kd_1 \to 0$. This result should be contrasted with the results obtained above when kd_1, $kd_2 \to 0$, where the instability configuration is case B or C provided $\rho_2 d_1^2 \neq \rho_1 d_2^2$.

To obtain more information on the instability configuration as a function of the dimensionless parameters kd_1, kd_2 and ρ_1/ρ_2, we have evaluated the stability boundaries $\lambda = 0$ and $\lambda = 2(\nu+\hat{\nu})|A|^2$ numerically. In order to facilitate comparison with the results of Part 2, these numerical results are presented in non-dimensional form, based on the lengthscale λ/π and timescale $(\lambda/\pi\alpha g)^{\frac{1}{2}}$, where $\alpha = (\rho_2-\rho_1)/(\rho_2+\rho_1)$ is the Boussinesq parameter. Here λ is the wavelength $2\pi k^{-1}$. The dimensionless parameters are now $D_{1,2} = \frac{1}{2}kd_{1,2}$ and α; the Boussinesq limit is $\alpha \to 0$, while when $\alpha \to 1$ we obtain the known results for a surface gravity wave (Benney & Roskes 1969; Hayes 1973; Davey & Stewartson 1974). All our results are displayed as graphs of the instability band in the (P, Q)-plane, with growth rates superimposed at selected values of P and Q; here P and Q are the non-dimensional variables $2\epsilon pk^{-1}$ and $2\epsilon qk^{-1}$ respectively. The non-dimensional growth rate is

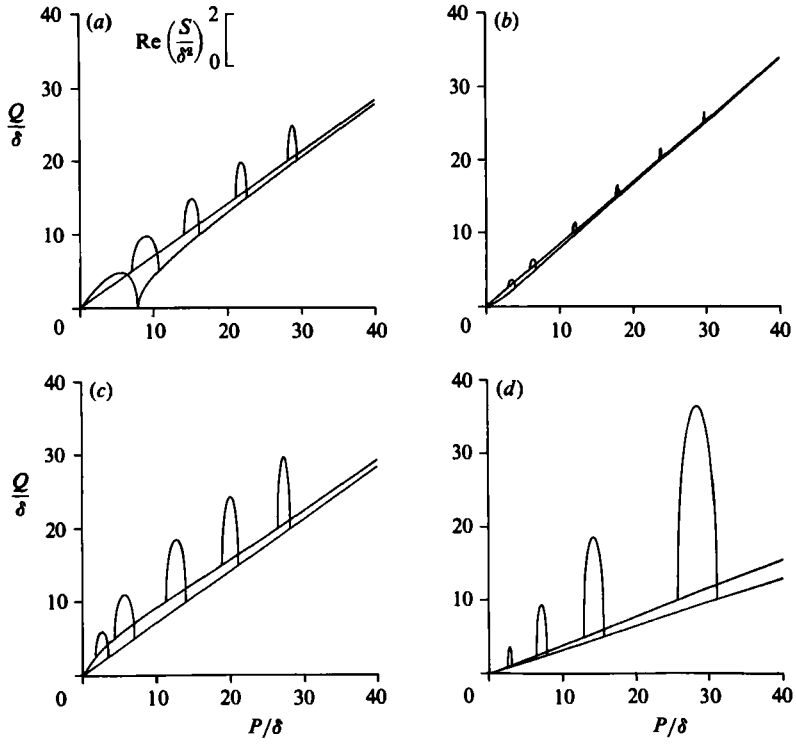

FIGURE 2. Stability boundaries and superposed growth rates (at Q = constant), $\alpha = 0$, $D_2 \to \infty$. (*a*) $D_1 = \pi$ [A]; (*b*) 0.225π [B]; (*c*) 0.1π [C]; (*d*) 0.025π [B]. Letters in square brackets refer to the instability-band configurations in figure 1.

$S = \epsilon^2 s(\frac{1}{2}k\alpha g)^{-\frac{1}{2}}$. Further, it is apparent from the expressions (4.3*b*), (4.4*b*) and (4.7) that P and Q scale with the non-dimensional amplitude $\delta = \epsilon k\,|A|$, while the growth rate S scales with δ^2. Hence our results are expressed in units of $P\delta^{-1}$, $Q\delta^{-1}$ and $S\delta^{-2}$, and for all the results shown the same scale is used.

In figure 2 we show the results when $\alpha = 0$ and $D_2 \to \infty$. This is the case discussed in Part 2, where we obtain the instability configuration for a range of wave amplitudes δ and modulation wavenumbers P, Q, thus extending the results obtained here, which are valid in the limit $\delta \to 0$ and P, $Q \to 0$. The results are shown for a range of values of D_1; as D_1 is decreased the instability configuration passes from case A to B when $D_1 = 0.75$, to case C when $D_1 = 0.60$, and returns to case B when $D_1 = 0.10$. The growth rates initially decrease with D_1, but later increase as $D_1 \to 0$. Note that case A shown in figure 2(*a*) is qualitatively similar to the deep-water limit D_1, $D_2 \to \infty$ discussed above (see the discussion following (4.9)). Also case B shown in figure 2(*d*) is qualitatively similar to the limit $D_1 \to \infty$, $D_1 \to 0$ discussed above (see the discussion following (4.19)).

In figure 3 we show the results when $\alpha = 0$ and $D_2/\pi = 0.1$ for a range of values of D_1 in order to give an indication of the effect of decreasing D_2 on the results shown in figure 2. In contrast with the case $D_2 \to \infty$ the instability is always transverse (i.e. there is no case A, which is the only case giving an instability in the wave direction). As D_1 is decreased the instability configuration passes from case C to D when $D_1 = 0.42$, returns to C when $D_1 = 0.23$, and finally becomes case B when $D_1 = 0.04$. The growth rates reach their maximum when $D_1 \approx D_2$ and decrease as $D_1 \to 0$. Note

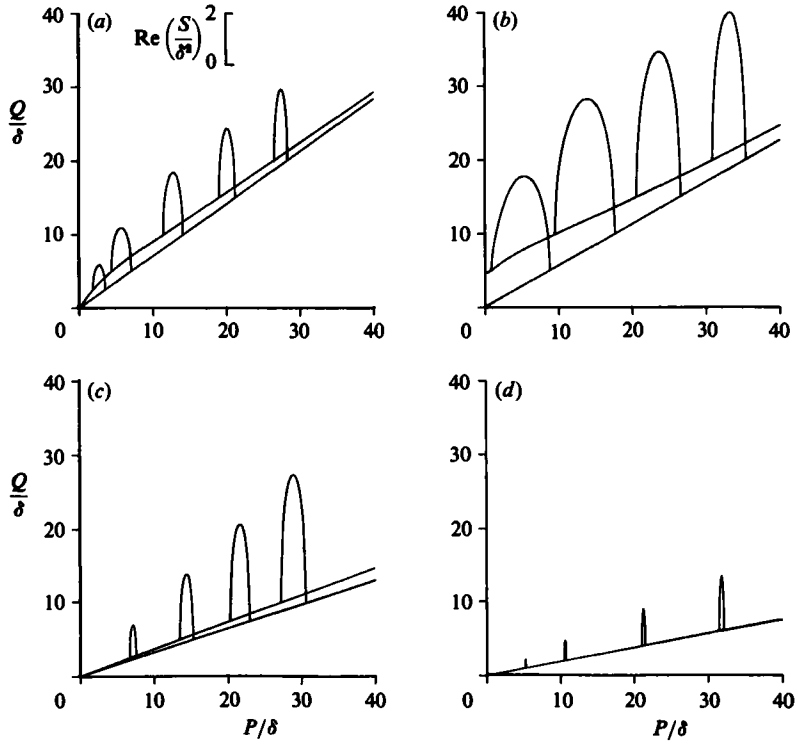

FIGURE 3. Stability boundaries and superposed growth rates (at Q = constant), $\alpha = 0$, $D_2 = 0.1\pi$. (*a*) $D_1 = \pi$ [C]; (*b*) 0.1π [D]; (*c*) 0.03π [C]; (*d*) 0.01π [B].

that case D in figure 3(*b*) is described by the analytical results above (see the discussion following (4.22)).

In figure 4 we show the results when $\alpha = 0.5$ and $D_2/\pi = 1.0$ for a range of values of D_1. Since the results for $D_2 \to \infty$ are similar to these, they provide an indication of the effect of increasing α on the results shown in figure 2. Overall the results are qualitatively similar to those shown in figure 2; in particular, the growth rates initially decrease with D_1 but later increase as D_1 is further decreased. The instability configuration is initially that for case A, but changes to case B when D_1 is decreased through the value $D_1 = 0.55$, to case C when $D_1 = 0.47$, and then to case D when $D_1 = 0.27$. This latter case is not present when $D_2 \to \infty$. Not shown in figure 4 are two further transitions to case C when $D_1 = 0.20$ and finally to case B when $D_1 = 0.04$. Note that case A shown in figure 4(*a*) is essentially that of the deep-water limit D_1, $D_2 \to \infty$ as discussed above (following (4.9)), while the final case B is essentially that for the limit $D_2 \to \infty$, $D_1 \to 0$ discussed above (following (4.19)).

In figure 5 we show the results when $\alpha = 0.9976$ and $D_1 \to \infty$, corresponding to an air–water interface with the upper fluid infinitely deep. These results, for a range of D_2, should be compared to the known results for a surface gravity wave (Benney & Roskes 1969; Hayes 1973; Davey & Stewartson 1974). Except for very small values of D_2, the results are very similar. As D_2 decreases, the growth rates decrease and the instability configuration passes from case A to case B when $D_2 = 0.69$, and then to case C when $D_2 = 0.19$. The corresponding transitions for a surface gravity wave are $D_2 = 0.68$ and $D_2 = 0.19$. Note that case A shown in figure 5(*a*) is for $D_2 \to \infty$ and is discussed above (following (4.9)). However, for the air–water interface there is a

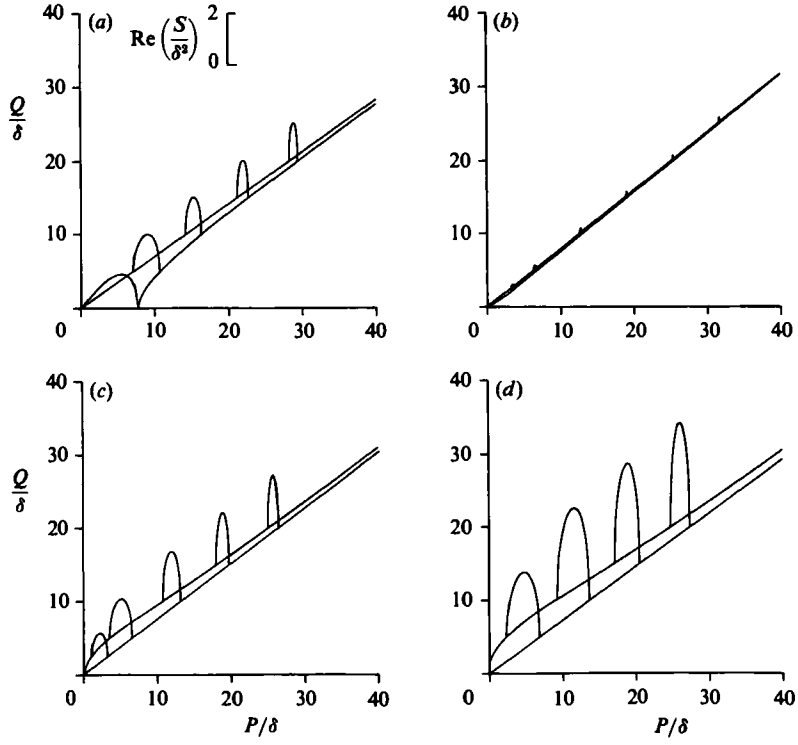

FIGURE 4. Stability boundaries and superposed growth rates (at Q = constant), $\alpha = 0.5$, $D_2 = \pi$. (*a*) $D_1 = \pi$ [A]; (*b*) 0.16π [B]; (*c*) 0.1π [C]; (*d*) 0.08π [D].

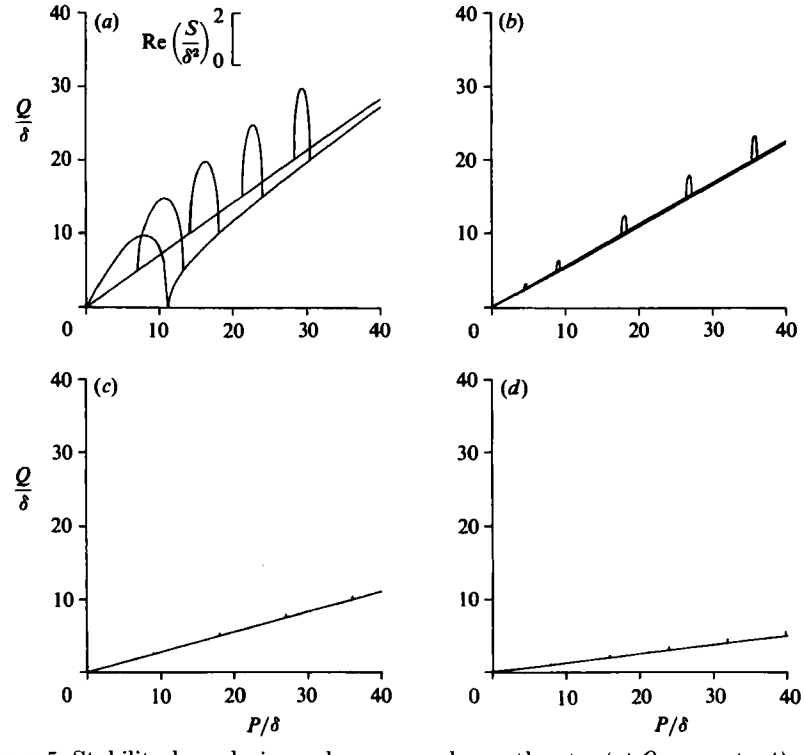

FIGURE 5. Stability boundaries and superposed growth rates (at Q = constant), $\alpha = 0.9976$ (air–water), $D_1 \to \infty$. (*a*) $D_2 \to \infty$ [A], (*b*) $D_2 = 0.1\pi$ [B]; (*c*) 0.045π [C]; (*d*) 0.025π [B].

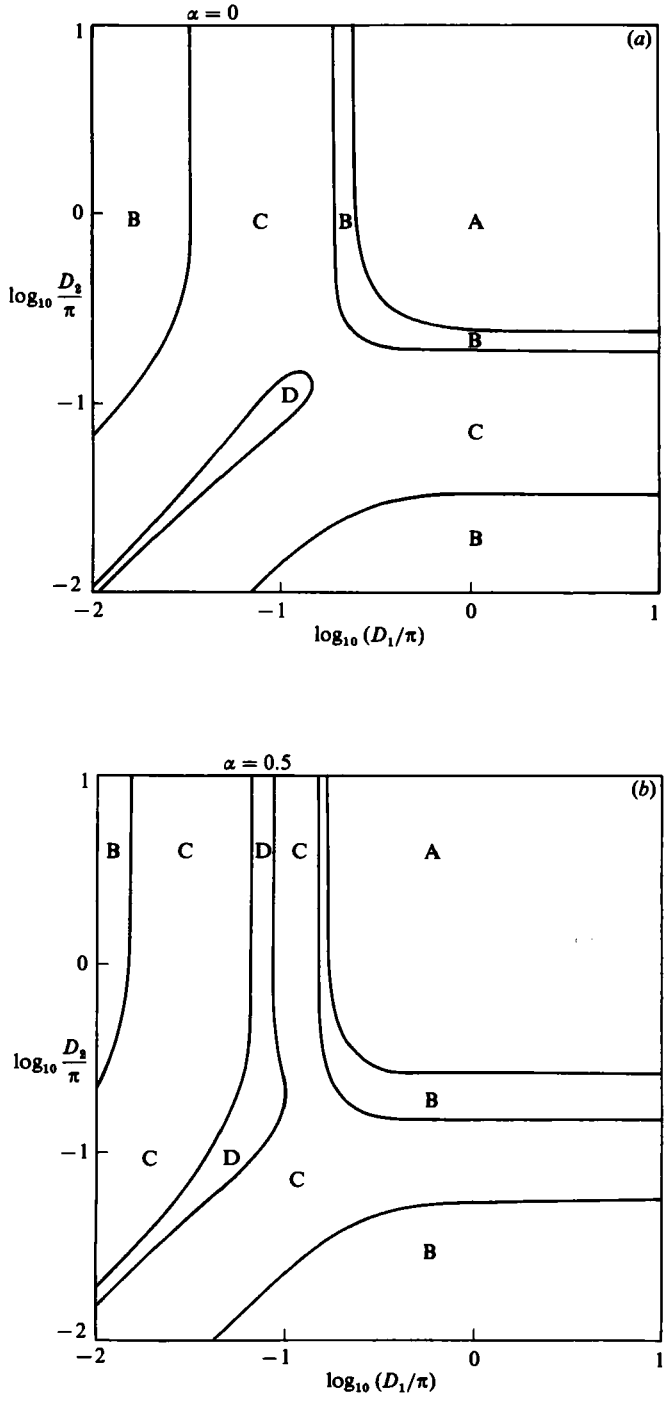

FIGURE 6. For caption see next page.

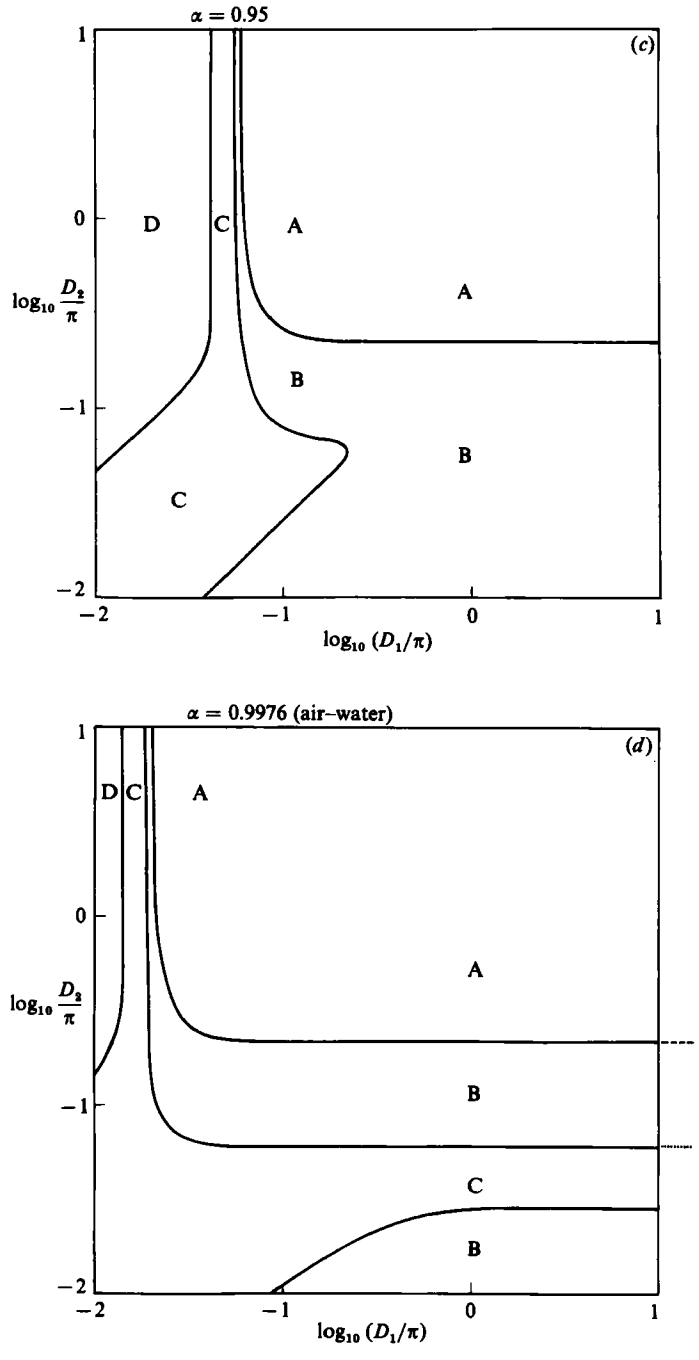

FIGURE 6. Instability regions in (D_1, D_2)-plane. (*a*) $\alpha = 0$; (*b*) 0.5; (*c*) 0.95; (*d*) 0.9976. Capital letters refer to the instability-band configurations of figure 1. The basic wave is modulationally stable on a B–C boundary. ---, A–B transition ($\alpha = 1$); · · · ·, B–C transition ($\alpha = 1$).

further transition from case C to case B when $D_2 = 0.09$, with a slight increase in growth rate (see figure 5*d*). This transition is not present for surface gravity waves. Its presence can be deduced, however, from the limit $D_1 \to \infty$, $D_2 \to 0$, which is analogous to the limit $D_2 \to \infty$, $D_1 \to 0$ discussed above (following (4.19)). From the results of this latter case it follows that when $D_1 \to \infty$, $D_2 \to 0$ the instability configuration is case B with finite growth rates for all non-zero values of ρ_1 (i.e. $\alpha \neq 1$). It follows that for surface gravity waves in very shallow water modulational instability is affected by the presence of the air above the fluid interface.

Many similar plots to those shown in figures 2–5 can be obtained. To provide an overview of these results as a function of the three parameters D_1, D_2 and α we show in figure 6 a plot of the instability case (A, B, C or D) as a function of D_1 and D_2 for various values of α. In interpreting these plots it is useful to recall the analytical results discussed above. In particular, $D_1, D_2 \to \infty$ produce case A, while $D_1, D_2 \to 0$ produce case B or case C provided $\rho_2 d_1^2 \neq \rho_2 d_1^2$. The limits $D_2 \to \infty$, $D_1 \to 0$ or $D_1 \to \infty$, $D_2 \to 0$ produce case B, while the case $\alpha = 0$, $D_1 = D_2$ gives a transition from A to B, to C and finally to D as D_1 is decreased. In figure 6(*a*) we show the case $\alpha = 0$, which is symmetric about $D_1 = D_2$. When D_1, D_2 both become large the instability configuration is case A and there is instability along the wave direction. As either D_1 or D_2 is decreased there is a transition to a transverse instability. Particularly interesting is the presence of a case-D region along the $(D_1 - D_2)$-axis, as case D includes a completely transverse instability, which does not occur for surface gravity waves. When α is increased the picture alters to that shown in figure 6(*b*) for $\alpha = 0.5$. The most significant change is the position of the case-D region. The consequences of further increases in α are shown in figure 6(*c*) for $\alpha = 0.95$ and 6(*d*) for $\alpha = 0.9976$ (corresponding to an air–water interface). Note that the case-D region continues to move to the upper left-hand corner where D_1 is small and D_2 is large, while the case-C region at first contracts to the right where D_1 is small, but then expands to the left where D_1 is large. The overall picture is not very sensitive to the value of α when α is small, but is extremely sensitive to the value of α as $\alpha \to 1$. When $\alpha = 1$ the picture is that for surface gravity waves and consists of a transition from case A to case B at $D_2 = 0.68$ and from case B to case C at $D_2 = 0.19$ with no dependence on D_1. These asymptotic limits are indicated on figure 6(*d*), where $\alpha = 0.9976$. It is apparent that for small D_2, and also for small D_1, there are significant differences from the case $\alpha = 1$.

5. Discussion

Our results in §4 show that a long-wavelength modulational instability exists for all values of the parameters α (i.e. $(\rho_2 - \rho_1)/(\rho_2 + \rho_1)$) and kd_1, kd_2. The instability occurs within an instability band in the (P, Q)-plane where (P, Q) is the non-dimensional modulation wavenumber. The analysis is restricted to small-amplitude waves and assumes that P, Q are $O(\delta)$, where δ is the non-dimensional measure of wave amplitude. The corresponding growth rates are $O(\delta^2)$ and the bandwidth is $O(\delta)$. The instability bands can be classified into the four cases shown in figure 1. The most notable distinction is between case A, which allows for an instability in the wave direction, and the remaining cases B, C and D, which allow only a transverse instability (i.e. $Q \neq 0$).

In part 2 we present numerical results for the linearized stability of finite-amplitude waves for the special case $\alpha = 0$ and $kd_2 \to \infty$. For this special case the numerical results extend and complement the analytical results obtained here. One of the main results obtained in Part 2 is that for small or moderate wave amplitudes the

modulational instability is part of a low-order resonance instability. This connection has been established for surface gravity waves by McLean *et al.* (1981), and is probably so for all cases of modulational instability discussed in this paper. For instance Yuen (1983) has obtained the same connection for the case when each layer is infinitely deep (d_1, $d_2 \to \infty$) and the density ratio ρ_1/ρ_2 is either 0.1 or 0.9. To demonstrate the generality of the connection, let $\omega(\boldsymbol{k})$ be the linear dispersion relation for the wave whose stability is being examined. Here $\boldsymbol{k} = (k, l)$ is the wavenumber, and $\omega(\boldsymbol{k})$ satisfies $D(\omega, k, l) = 0$ (see (2.5*b*)). For $\delta \approx 0$ this wave will be unstable owing to a resonant interaction with two other waves with wavenumbers $\boldsymbol{k}_1$, $\boldsymbol{k}_2$ and frequencies $\omega_1 = \omega(\boldsymbol{k}_1)$, $\omega_2 = \omega(\boldsymbol{k}_2)$ whenever

$$\boldsymbol{k}_2 - \boldsymbol{k}_1 = N\boldsymbol{k}, \quad \omega_2 - \omega_1 = N\omega. \tag{5.1}$$

Here N is a positive integer and defines the order of the resonance. We expect the growth rates of the instability to be $O(\delta^N)$. When $N = 1$ the resonance condition (5.1) describes a triad resonance. However, for the interfacial waves being considered here it can be shown that there are no resonant triads. The argument is similar to that used for surface gravity waves (see Phillips 1960) and is based on the fact that the group velocity V is always less than the phase velocity c in absolute value.

The resonance condition (5.1) can be met for $N \geqslant 2$. In particular, the $N = 2$ resonance exists, and corresponds to a quartet resonance. For the special case discussed in Part 2 the locus of wavenumbers $\boldsymbol{k}_1$ that satisfy (5.1) for a fixed $\boldsymbol{k}$ can be shown to form a figure-of-eight (see figure 1 of Part 2). Further, the $N = 2$ resonance contains the modulational instability in the following sense. Let $\boldsymbol{k} = (k, 0)$ and $\boldsymbol{k}_2 = k(1 + \frac{1}{2}P, \frac{1}{2}Q)$, $\boldsymbol{k}_1 = k(-1 + \frac{1}{2}P, \frac{1}{2}Q)$ and note that $P = 2\epsilon p k^{-1}$ and $Q = 2\epsilon q k^{-1}$. Here ϵ is a small parameter measuring the magnitude of the modulation wavenumber. For small ϵ the resonance condition (5.1) for $N = 2$ is approximately given by, to $O(\epsilon^2)$,

$$\lambda_1 p^2 + \lambda_2 q^2 = 0, \tag{5.2}$$

where $\lambda_{1,2}$ are defined by (4.1*c*). From (4.4*b*) we see that (5.2) is equivalent to $\lambda = 0$, and thus coincides with one of the modulational instability boundaries. Of course, the resonance condition (5.1) is exact only for $\delta = 0$. For small but finite δ the resonance instability develops a finite bandwidth in the (P, Q)-plane, but closely follows the curve defined by (5.1). Further, near the origin of the (P, Q)-plane (i.e. as $\epsilon \to 0$) the resonance instability for $N = 2$ can be identified with the modulational instability. Our results in Part 2 show that for the case $\alpha = 0$ and $kd_2 \to \infty$ the higher-order resonances ($N \geqslant 3$) also occur, but that for small or moderate amplitudes the dominant instability is that corresponding to $N = 2$.

REFERENCES

Benney, D. J. & Newell, A. C. 1967 The propagation of nonlinear wave envelopes. *J. Maths & Phys.* **46**, 133–139.

Benney, D. J. & Roskes, G. J. 1969 Wave instabilities. *Stud. Appl. Maths* **48**, 377–385.

Davey, A. & Stewartson, K. 1974 On three-dimensional packets of surface waves. *Proc. R. Soc. Lond.* A **338**, 101–110.

Grimshaw, R. 1981 Modulation of an internal gravity wave packet in a stratified shear flow. *Wave Motion* **3**, 81–103.

Grimshaw, R. 1984 Solitary waves in slowly varying environments: wave packets. In *Advances in Nonlinear Waves* (ed. L. Debnath), pp. 38–58.

Hayes, W. D. 1973 Group velocity and nonlinear dispersive wave propagation. *Proc. R. Soc. Lond.* A **332**, 194–221.

McLean, J. W. 1982*a* Instabilities of finite-amplitude water waves. *J. Fluid Mech.* **114**, 315–330.

McLean, J. W. 1982*b* Instabilities of finite-amplitude waves on water of finite depth. *J. Fluid Mech.* **114**, 331–341.

McLean, J. W., Ma, Y. C., Martin, D. U., Saffman, P. G. & Yuen, H. C. 1981 Three-dimensional instability of finite-amplitude water waves. *Phys. Rev. Lett.* **46**, 817–820.

Phillips, O. M. 1960 On the dynamics of unsteady waves of finite amplitude. Part 1. The elementary interactions. *J. Fluid Mech.* **9**, 193–217.

Pullin, D. I. & Grimshaw, R. H. J. 1983*a* Nonlinear interfacial progressive waves near a boundary in a Boussinesq fluid. *Phys. Fluids* **26**, 897–905.

Pullin, D. I. & Grimshaw, R. H. J. 1983*b* Interfacial progressive waves in a two-layer shear flow. *Phys. Fluids* **26**, 1731–1739.

Pullin, D. I. & Grimshaw, R. H. J. 1985 Stability of finite-amplitude interfacial waves. Part 2. Numerical results. *J. Fluid Mech.* **160**, 317–336.

Whitham, G. B. 1974 *Linear and Nonlinear Waves.* Wiley.

Yuen, H. C. 1983 Instability of finite-amplitude interfacial waves. In *Waves on Fluid Interfaces* (ed. R. E. Meyer), pp. 17–40. Academic.

Zakharov, V. E. 1968 Stability of periodic waves of finite amplitude on the surface of a deep fluid. *Sov. Phys. J. Appl. Mech. Tech. Phys.* **4**, 190–194.